ELSEVIER

Coordination Chemistry Reviews
174 (1998) 343–359

COORDINATION CHEMISTRY REVIEWS

Accordion porphyrins
Hybrid models for heme and binuclear monooxygenases[1]

W. Alexander Reiter, Aida Gerges, Shaoyung Lee, Tamboue Deffo, Thomas Clifford, Andrew Danby, Kristin Bowman-James *

Department of Chemistry, University of Kansas, Lawrence, KS 66045, USA

Received 24 October 1997; received in revised form 2 March 1998; accepted 20 April 1998

Contents

* Corresponding author. Fax: +1 785 864 5396; e-mail: kbowmanjames@caco3.chem.ukans.edu

[1] This paper is dedicated to Professor Daryle H. Busch, a revered colleague, friend, and mentor, on the occasion of his seventieth birthday. The idea for the "accordion porphyrin" originated after a phone conversation between K.B.-J. and Professor Busch almost 20 years ago. The subject of the conversation concerned exploring binuclear complexes as catalysts. Professor Busch's advice was to design a totally new ligand, which started thought processes about Nature's catalysts. While the original metal complexes were not successful catalysts, our more recent discoveries with regard to the manganese complexes have been rewarding. K.B.-J. would like to thank Professor Busch for that very sage advice.

0010-8545/98/$ – see front matter
PII S0010-8545(98)00118-0

Abstract

The synthesis, characterization, and examination of the monooxygenase activity of tetrapyrrolic macrocyclic complexes with an accordion porphyrin-like ligand framework are described. Cyanovinyl protection techniques were used to obtain a diformyl dipyrromethane, which was condensed with 1,3-diaminopropane in the presence of metal acetate template to achieve manganese(II), nickel(II), and copper(II) complexes. The macrocycle was found to be in the dipyrromethene form for both the manganese(II) and copper(II) complexes, and in the dipyrromethane form for the nickel(II) complex. The crystal structure of the acetate salt of the manganese(II) complex was obtained. The manganese(II) complex was found to catalyze the epoxidation of cyclohexene, yielding primarily the epoxide (40%) with only minor side products, while the nickel(II) and copper(II) complexes showed little catalytic activity. A lack of stereoselectivity was observed in the epoxidation of *cis*- and *trans*-stilbene by the manganese(II) complex, which yielded only *trans*-epoxide in the reaction with *trans*-stilbene, but both *cis* and *trans* products in the reaction with *cis*-stilbene.

Keywords: Manganese; Accordion porphyrin; Binuclear; Metalloporphyrin model; Cytochrome P450 model; Monooxygenase model

1. Introduction

Oxygen chemistry plays a major role in biological processes. For example, molecular oxygen must be activated in order to be incorporated into other biomolecules; hydrogen peroxide and superoxide ion need to be detoxified; and ultimately, life as we know it is dependent on the regeneration of molecular oxygen by photosynthesis. Closely associated with each of these processes are metalloenzymes which are capable of efficient handling of dioxygen species. Two key types of metalloproteins involved in oxygen chemistry recur in biological systems, heme-based proteins with highly versatile porphyrin frameworks, and dinuclear metalloproteins with two metal sites often separated by bridging carboxylates [1–9]. In the heme proteins, iron is clearly the metal of choice. The binuclear metalloproteins are more "liberal" with respect to metal ion, however, and diiron, dicopper, and dimanganese proteins, as well as mixed metal protein sites, can be found. Hence, there are clearly characteristics inherent in both the binuclear and heme frameworks that impart the appropriate catalytic and/or binding capabilities with respect to dioxygen and dioxygen-containing species. The specific catalytic event which is the subject of this paper is the activation of C–H bonds, i.e. monooxygenase activity.

The activation of the C–H bond for incorporation of oxygen has been the focus of much effort [10,11], and some of the more prominent catalysts in this area are the heme-containing enzymes, the cytochromes P450 [12,13]. Structural aspects of the cytochromes P450 are well established [14], with proposed catalytic cycles including a high-valent iron oxo species [12]. Considerable success in mimicking cytochrome P450 activity has been obtained with model compounds, many of which involve porphyrin-derived complexes [11,15]. Yet binuclear metalloenzymes, includ-

ing the dicopper enzyme tyrosinase [16] and the diiron enzyme methane monooxygenase [17], also display cytochrome P450-type monooxygenase activity. Fig. 1 shows the salient features of the metal coordination sites of the three metalloenzymes [14,16,18–20].

Tyrosinase catalyzes the *o*-hydroxylation of monophenols, a process known as cresolase activity, and also the two electron oxidation of *o*-diphenols to *o*-quinones

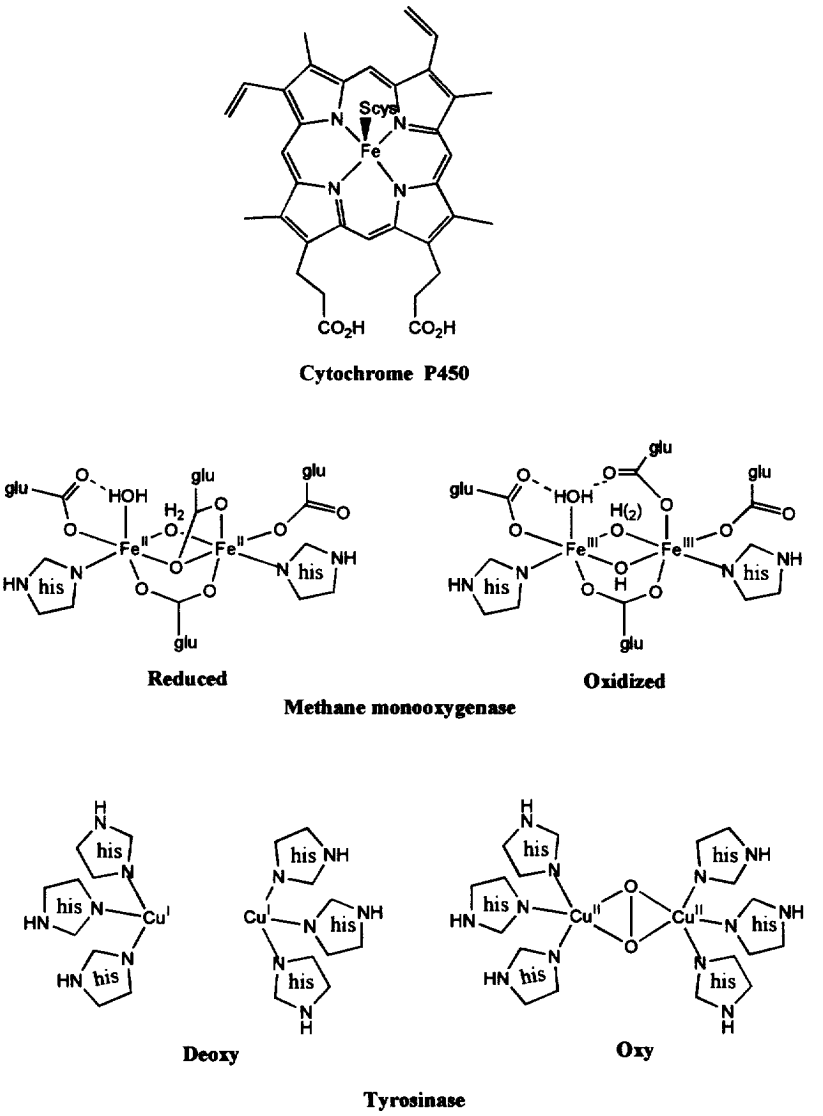

Fig. 1. Active sites for cytochrome P450, methane monooxygenase, and tryosinase.

[16]. Unfortunately, crystal structures of the enzyme are not available to define unequivocally the active site during the various stages of catalysis. Nonetheless, X-ray absorption spectroscopy data [18] and comparison with the active site of hemocyanin (considered to be a "descendent" enzyme with a similar active site) have given an indication of the species and active site involved in tyrosinase [16]. These include three-coordinate (histidine ligands) copper(I) environments in deoxytyrosinase, five-coordinate copper(II) sites in oxytyrosinase with a side-on μ-η^2:η^2 peroxide, and Cu–Cu distances of about 3.4 Å.

The diiron-containing methane monooxygenase, which catalyzes the transformation of methane to methanol [17], has been structurally characterized [19,20], and interestingly the active site is very similar to that of ribonucleotide reductase [21,22], a key enzyme in DNA biosynthesis, but dissimilar to hemerythrin [23], the oxygen transport protein in invertebrates. Methane monooxygenase consists of three components, with the diiron site contained in the monooxygenase (or hydroxylase) component. The active site of the reduced form consists of two iron(II) atoms each coordinated to a histidine and carboxylate, and bridged by two other carboxylates. One of the bridging carboxylates shifts to a terminal coordination mode upon oxygen binding. This type of "carboxylate shift " has been cited as potentially playing a critical role in the catalytic activity involved with oxygen activation [24].

Our design of the binucleating "accordion" porphyrin **1** a number of years ago [25–28] was based on the desire to incorporate aspects of the porphyrin framework into a binuclear environment, and to explore whether such complexes could be effective catalysts and "models" for enzymes such as the cytochromes P450 and the dinuclear monooxygenases. The synthesis of the 5,5′-diformyl dipyrromethane precursor to the accordion-like complexes is somewhat tedious, however, and we sought to develop a more facile synthetic route. This was accomplished via the use of cyanovinyl protection [29,30] of commercially available pyrrole carboxaldehyde. The protected pyrrole can be readily condensed with benzaldehyde followed by deprotection to yield the precursor dialdehyde via a three step route. Complexes of the phenyl derivative, **2**, can then be synthesized by template-assisted Schiff base condensations.

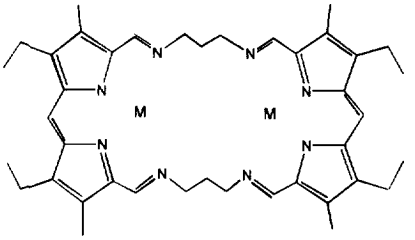

1

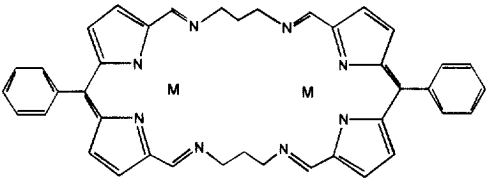

2

Our initial goal was to examine the resulting binuclear complexes for monooxygenase activity. We followed the cytochrome P450 model routes examining the propensity of the complexes to catalyze the oxidation of cyclohexene and *cis*- and *trans*-stilbene using iodosylbenzene as a source of oxygen. While nickel(II) and copper(II)

complexes displayed little or no catalytic activity with these substrates, dimanganese(II) complexes did show significant aptitude for the epoxidation of olefins. The tetrapyrrolic ligand system was found to have extremely flexible coordination properties, as evidenced by the crystal structures of the dicopper(II) structure with **1** reported earlier [26] and the dimanganese(II) structure of **2** reported here. This paper describes the synthesis and characterization of the dicopper(II), dinickel(II), and dimanganese(II) complexes, **2**, the crystal structure of the acetate salt of the dimanganese(II) complex of **2**, and monooxygenase catalytic studies of these complexes.

2. Synthesis

As noted above, 5,5′-diformyl-substituted dipyrromethanes, the crucial precursors for the synthesis of the desired macrocycles, are not readily available. The successful use of methyl cyanoacetate as a protecting reagent for the commercially available pyrrole-2-carboxaldehyde provides for a more efficient synthetic route. As shown in Scheme 1, the dipyrromethane portion of the macrocycle can be readily synthesized in three steps, much preferable to the longer eight step "from scratch" synthesis. As

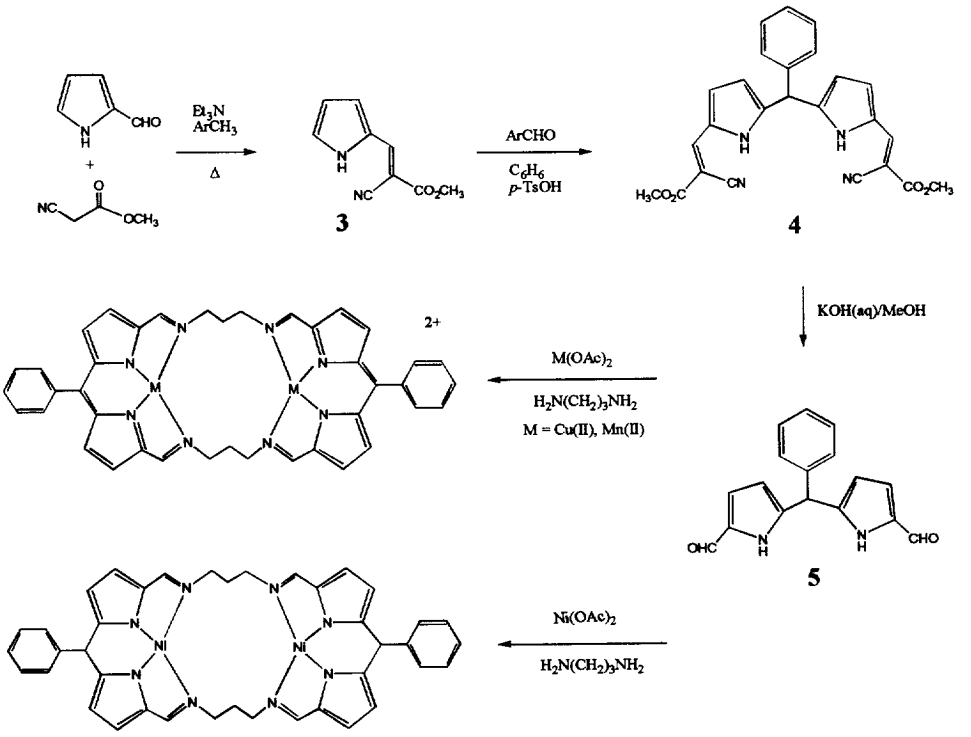

Scheme 1.

a precautionary measure all of the reactions were done under N_2 atmosphere. The desired protected pyrrole, **3**, was obtained by a modified procedure of Dolphin [29,30], in which pyrrole-2-carboxaldehyde was reacted with methyl cyanoacetate in toluene. The yellow product was then condensed with benzaldehyde in a manner similar to that described by others [31]. The condensation is carried out with a large excess of benzaldehyde, and for short periods only. While the protection step can be carried out in toluene, the condensation with benzaldehyde does not proceed when toluene is used. This particular step is critical, and if the reaction is run for too long a time, messy tars are obtained. Hence, the yield for this reaction varies considerably depending on the reaction time. (We have noted that electron withdrawing groups on the benzaldehyde tend to facilitate this condensation, but make the final deprotection step more difficult [32].) The condensation product, **4**, was then deprotected by refluxing in 10 M NaOH.

Formation of the macrocyclic metal complexes was accomplished by using the appropriate metal acetate salt as a templating agent for a Schiff base reaction between the 5,5′-diformyl-dipyrromethane and 1,3-diaminopropane. The dipyrromethane portion of the macrocycle, which usually oxidizes to the dipyrromethene form upon exposure to air [25,26], was found to be more stable with the phenyl substitution, and only the manganese(II) and copper(II) complexes were isolated as acetate salts. The nickel(II) complex was obtained in the neutral dipyrromethane form.

3. Physical properties

3.1. Crystal structure of $[Mn_2 \cdot 2](OAc)_2$

The crystal structure of the dimanganese complex **2** shows an interesting coordination environment around the two manganese ions (Fig. 2). Each manganese is coordinated to the macrocycle via two $Mn–N_{pyrrole}$ and two adjacent $Mn–N_{imine}$ bonds. However, the four $Mn–N_{imine}$ bonds are considerably elongated, ranging from 2.41 to 2.49 Å. Of particular note are the presence of a coordinated acetate, a very weakly bound, chelated acetate [Mn–O = 2.40(1) Å and 2.42(1) Å], as well as a bound water molecule [Mn–O = 2.162(7) Å]. The presence of the surrounding carboxylates and the coordinated water molecule make the coordination environment not unlike that found in a number of dimanganese metalloproteins [2–4,7,8]. However, the Mn–Mn distance is 5.40 Å, which is somewhat longer than that found for most of the bimetallic manganese proteins. A clearer view of the coordination environment of the manganese ions is shown in Fig. 3, where the *syn–anti* conformation of the bridging acetate is clearly seen as well as the position of the weakly bound acetate.

The dipyrromethene fragments are essentially planar, and the manganese ion is located in the plane (deviations of 0.045 and −0.014 Å); however, the imines are tilted from these planes by amounts ranging from 0.108 to 0.294 Å. As can be seen in Fig. 3 it is also apparent that both groups of four nitrogen atoms form square

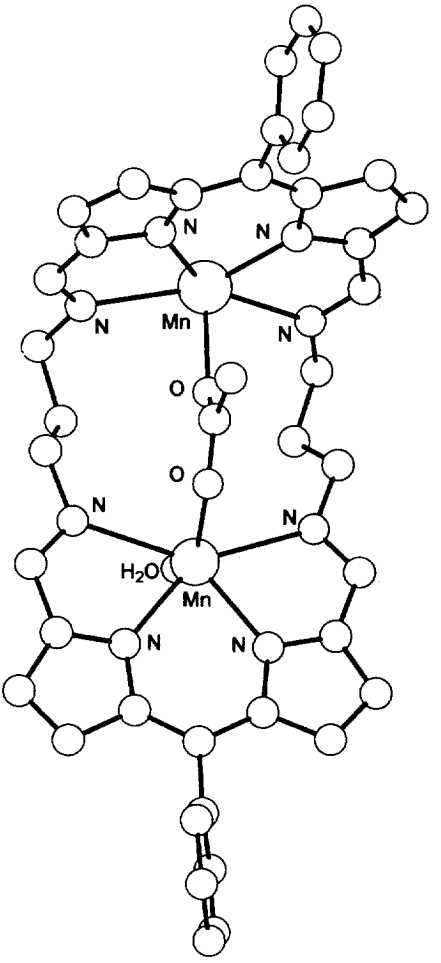

Fig. 2. Perspective view for the dimanganese(II) complex, **2**. The weakly chelated acetate is omitted for clarity.

planar arrays around their respective manganese ions. Almost identical results are obtained if the manganese is excluded from the plane calculations. Interestingly, one of the appended phenyl groups is almost perpendicular to its dipyrromethene neighbor (95.7°), while the other is slightly visibly canted, with an angle of 101.0° to its dipyrromethene plane.

To date this is the second crystal structure of a transition metal complex with the "accordion-like" binucleating porphyrin. The first crystal structure of the copper(II) azido complex with **1**, reported in 1985, indicated a rather unusual twisting of the macrocycle and a totally different coordination mode (Fig. 4) [26]. In the copper(II) case, the two dipyrromethene fragments are aligned in a "face-to-face" orientation,

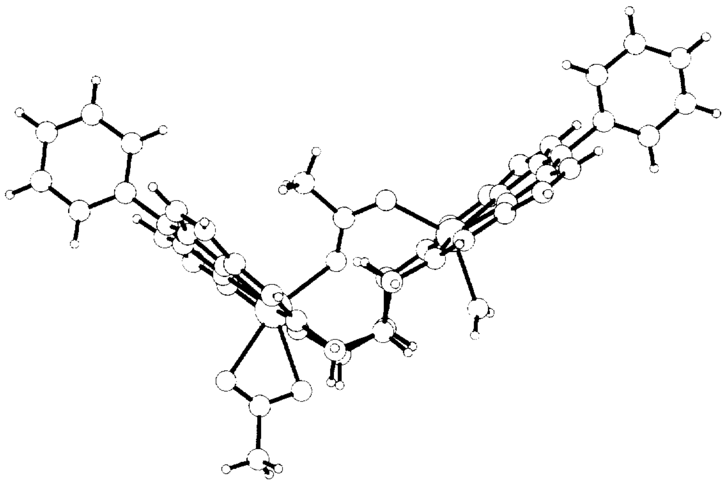

Fig. 3. Side view of the dimanganese(II) complex, **2**, showing the *cis,anti* conformation of the bridging acetate, the weakly chelated acetate, and the coordinated water molecule.

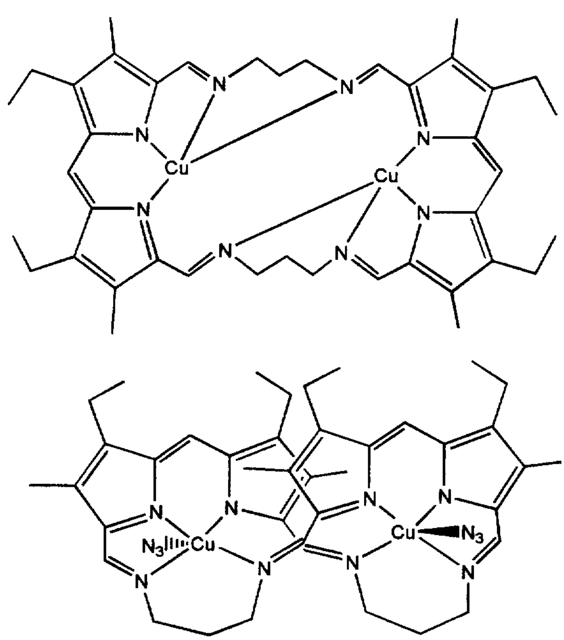

Fig. 4. Drawing of the bonding scheme and approximate structure of $[Cu_2 \cdot \mathbf{1}](N_3)_2$.

yet the copper ions are still relatively distant at 5.39 Å. Two azides are coordinated to the copper in end-on (monodentate) fashions, making each copper ion five-coordinate, in a distorted bipyramidal environment. Hence, the coordination possi-

bilities for this macrocycle are varied, and evidence is accumulating that this can and does influence the chemistry of these complexes.

3.2. Electronic spectra

The flexibility of the ligand with respect to coordination modes also seems to affect the physical properties of the resulting complexes. Both the manganese and copper complexes have similar UV–vis spectra, with two intense bands in the visible region at 542 nm ($\log \epsilon = 4.47$) and 568 nm ($\log \epsilon = 4.41$) for the dimanganese complex and 552 nm ($\log \epsilon = 3.93$) and 590 nm ($\log \epsilon = 3.92$) for the dicopper complex [Fig. 5(A, B)]. The intense observed bands are most probably related to metal to ligand charge transfer bands involving the conjugated system as observed for dipyrromethene [33,34] and porphodimethene complexes [35]. These bands are clearly absent in the dinickel complex, for which the lowest energy band is at 432 nm ($\log \epsilon = 3.94$) [Fig. 5(C)].

The spectrum of the dimanganese complex with **2** is also solvent dependent (as noted previously for several of the copper(II) complexes with **1**) [26]. In anhydrous methanol the two intense absorptions at 542 and 568 nm decrease as water is added, giving rise to a weaker band at 510 nm, and the color changes from the intense violet to a lighter reddish purple (Fig. 6). The interesting dependence of the electronic spectrum on water seen for the manganese complex is not observed for other metal complexes and is being investigated further. It is possible that the spectral changes may be related to hydration effects with a shift in coordination from the "twisted" macrocycle as seen in the copper structure (Fig. 4) to the more open structure observed for the dimanganese(II) complex with coordinated water (Figs. 2 and 3).

4. Monooxygenase activity

The oxidation results for the manganese, copper, and nickel complexes of **2** are summarized in Table 1, in comparison with data previously reported for other catalysts. While it is not appropriate to make strict comparisons of data because of differences in reaction conditions and stoichiometries, it is interesting to note the definite trends for mononuclear porphyrins and macrocycles, as opposed to binuclear systems. Also it should be noted that this is not meant to be a comprehensive review of all of the work that has been done with respect to oxidation catalysts. The compounds chosen for comparisons are the simple porphyrins and selected representative non-porphyrin complexes of macrocyclic or binuclear nature.

4.1. Cyclohexene epoxidations

For cyclohexene epoxidation reactions (Table 1), it is clear that the dimanganese(II) complex is really the only viable catalyst of the three complexes examined with ligand **2**. The overall yield for $(Mn_2 \cdot \mathbf{2})^{2+}$ was 40% epoxide with only minor amounts of the hydroxide and ketone (4% and 3%, respectively). The

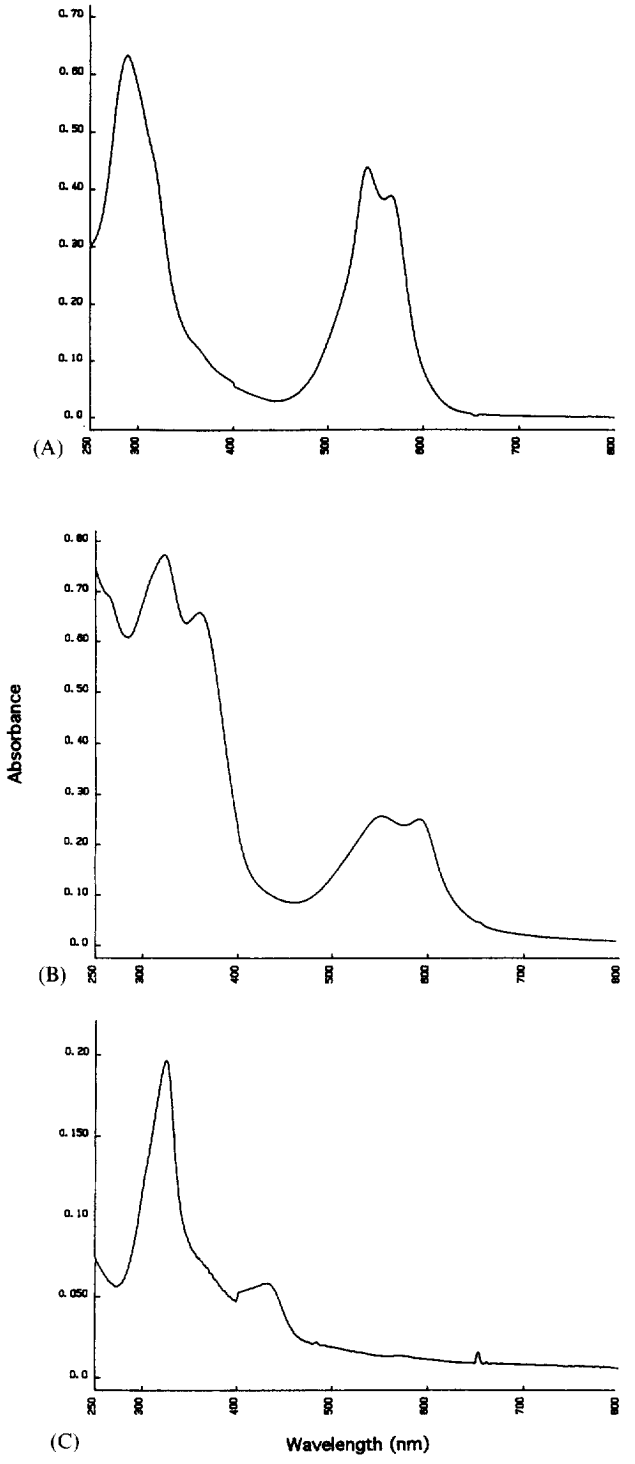
Absorbance
Wavelength (nm)
(A)
(B)
(C)

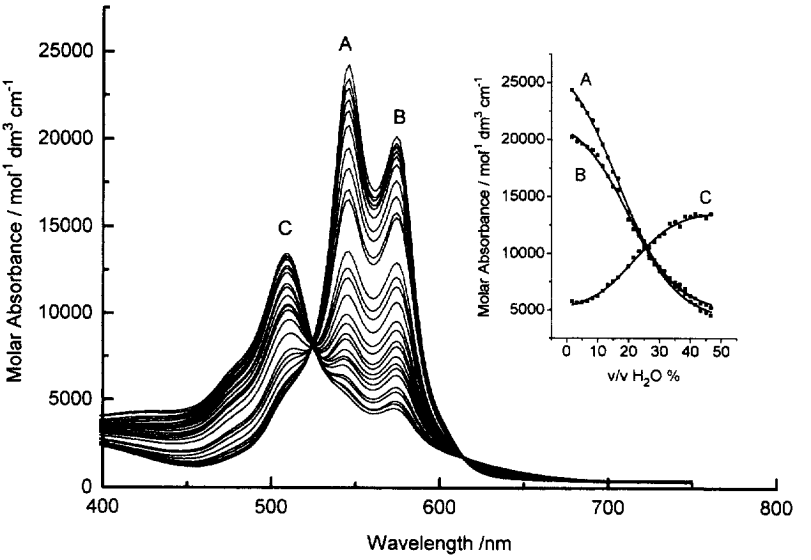

Fig. 6. UV–vis absorption spectra of $[Mn_2 \cdot \mathbf{2}](OAc)_2$ (5.75×10^{-5} M) in a CH_3OH:H_2O mixture ranging from 0 to 50% H_2O v/v illustrating the decrease in the absorptions at 546 and 574 nm and increase of the absorption at 510 nm with increased percentage of H_2O at 21°C. Inset shows the molar absorbances found at the peaks 510 (C), 546 (A), and 574 nm (B) vs. % H_2O.

finding that only the dimanganese(II) complex with **2** was active probably relates to the propensity for manganese to form high-valent manganese-oxo species. Of the selection chosen for comparison, Fe(TTP)Cl gave the best catalytic yield of the epoxide at 67%, but also 15% of the hydroxylated product [36]. Structures for the non-porphyrin ligands are shown in Fig. 7. Ni(cyclam)$^{2+}$ (Ni·**6**) gave the largest yield for the hydroxide (34%) along with considerable amounts of the epoxide (25%) and a small amount of the ketone (10%) [37,38]. What is quite interesting, however, is the product distribution for the mononuclear manganese(III) complexes (Mn·**7** and Mn·**8**) [39,40] and copper(II) binuclear catalysts ($Cu_2 \cdot$**9**–$Cu_2 \cdot$**11**) [41] as well as for $Mn_2 \cdot$**2**. These catalysts all give predominantly the epoxide and only minor amounts of the side products, which could point to mechanistic similarities in the binuclear catalysts.

4.2. Stilbene epoxidations

In the reaction with *cis*- and *trans*-stilbene, there is also considerable difference between the binuclear and mononuclear catalysts. The $Mn_2 \cdot$**2** complex reacts with both *cis*- and *trans*-stilbene. In the *cis*-stilbene reaction, both *cis*- and *trans*-epoxides

Fig. 5. Absorption spectra in CH_2Cl_2 of (A) $[Mn_2 \cdot \mathbf{2}](OAc)_2$ (1.5×10^{-5} M), (B) $[Cu_2 \cdot \mathbf{2}](OAc)_2$ (3.0×10^{-5} M), and (C) $[Ni_2 \cdot \mathbf{2}]$ (6.7×10^{-6} M).

Table 1
Comparison of the percentage yields of oxidation products of cyclohexene with $Mn_2 \cdot 2^{2+}$ and selected porphyrin, binuclear copper and macrocyclic nickel catalysts in the presence of iodosyl benzene.

	Yield (%)		
	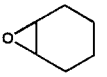	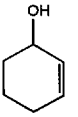	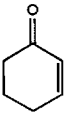
$Mn_2 \cdot 2^{2+}$	40	4	3
$Cu_2 \cdot 2^{2+}$	2	0.7	0.6
$Ni_2 \cdot 2$	1	0.4	0.9
Fe(TPP)Cl[a]	55	15	—
Fe(TTP)Cl[a]	67	15	—
FePPIX-DME[a]	22	5	—
Ni · 6[b,c]	25	34	10
Mn · 7[c,d]	58	—	—
Mn · 8[c,e]	46	2[f]	—
$Cu_2 \cdot 9$[c,g]	19	<1	4
$Cu_2 \cdot 10$[c,g]	23	<1	3
$Cu_2 \cdot 11$[c,g]	24	—	—

[a] Ref. [36]. In CH_2Cl_2. Abbreviations: TPP, *meso*-tetraphenylporphyrin; TTP, *meso*-tetra-*o*-tolylporphyrin; PPIX-DME, protoporphyrin IX dimethyl ester.
[b] Refs. [37,38]. In CH_2Cl_2.
[c] Structures **6–11** can be found in Fig. 7.
[d] Ref. [39]. In CH_3CN.
[e] Ref. [40]. In methanol.
[f] Cyclohexenyl methyl ether.
[g] Ref. [41]. In CH_3CN.

are isolated (15.2% and 9.0% yield, respectively). In the reaction with *trans*-stilbene, only the *trans*-epoxide is isolated (34.5% yield). Since little activity was observed for the copper and nickel complexes of **2** with cyclohexene epoxidation, these complexes were not examined further. For comparison, however, Fe(TPP)Cl is highly stereospecific, reacting preferably with *cis*-stilbene, giving only *cis* product. It has been proposed that the phenyl groups on the porphyrin ring facilitate the reaction by non-bonding interactions with the substrate. This theory was cited as being supported by the findings for the same reaction with the iron complex with protoporphyrin IX, which shows significantly decreased catalytic capabilities [36]. On the contrary, in the dicopper ($Cu_2 \cdot 9$) reactions with both *cis*- and *trans*-stilbene, only *trans* products in fairly low yields were isolated [41]. It has been noted in manganese porphyrin epoxidations that stereospecificity in *cis*-alkene reactions is the result of a Mn(V)=O species, while a Mn(IV)=O species results in a lack of stereospecificity [42,43]. Considering the lack of stereospecificity in the $Mn_2 \cdot 2$ case, it may be tentatively suggested, based on the previous findings with manganese porphyrins, that a Mn(IV)=O species is the active catalyst. It has also been

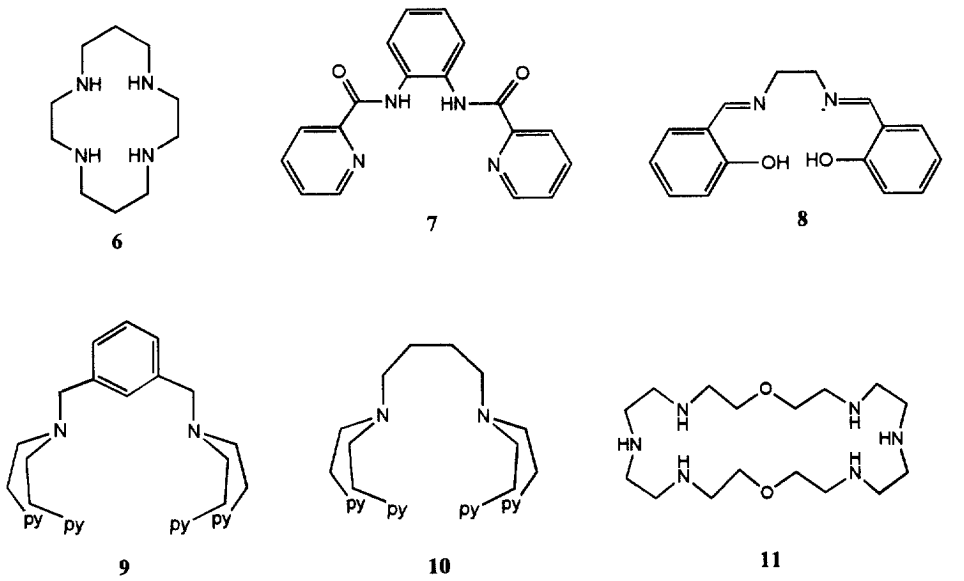

Fig. 7. Ligands for which monooxygenase activity has been reported by other workers (Table 1).

proposed that μ-oxo manganese(IV) species are involved in these oxidations [40,44,45], which is a possibility.

4.3. Summary of monooxygenase activity

It is clear that the dimanganese(II) complexes with the "accordion" porphyrin are capable of catalyzing monooxygenase reactions and as such are hybrid models for both heme and binuclear monooxygenase enzymes. The reactions do not proceed in the absence of an oxygen source such as iodosyl benzene. The mechanism of the reactions is still not clearly understood, although the formation of high-valent manganese oxo species or a complex with bridging oxo groups are likely possibilities. We are currently continuing investigations in the area of binuclear catalysts with interest in achieving higher stereoselectivities as well as asymmetric syntheses.

5. Experimental section

5.1. Physical measurements

NMR spectra were obtained on a Varian XL-300 spectrometer using TMS as an internal standard. Mass spectral data were obtained by Dr. T. Williams of the Mass Spectrometry Laboratory at the University of Kansas on a ZAB HS mass spectrometer equipped with an 11/250 data system. FAB mass spectrometry experiments (usually in nitrobenzyl alcohol, NBA) were performed using a xenon gun operated

at 8 k eV energy and 0.8 mA emission. Elemental analysis for carbon, hydrogen and nitrogen was performed at the Microanalytical Laboratory, University of Kansas, by Dr. Tho Nguyen and at Midwest Microlab, Indianapolis, IN. A Hewlett Packard 8450A diode array and a Schimadzu SPC 2100 spectrophotometer were used to obtain UV–vis spectra. Gas chromatographic analyses were done using a Hewlett Packard 5890A gas chromatograph with an FID detector and an HP-17 column.

5.2. Synthesis

All the chemicals used were reagent grade or better. Cyclohexene used in oxidation studies was gold label and stored over $CaCl_2$. CH_2Cl_2 used for the oxidation studies was HPLC grade, dried over $MgSO_4$ and deaerated with argon. Iodosylbenzene was synthesized by published methods [46].

5.2.1. Synthesis of macrocycle precursors

Methyl(E)-2-cyano-3-(2-pyrrolyl)-propenate (**3**). In a 2 l flask fitted with a Dean Stark trap pyrrole-2-carboxaldehyde (40.6 g, 0.416 mol) and ethylcyanoacetate (43 g, 0.432 mol) were dissolved in toluene (1 l). Triethylamine (10 ml) was added as catalyst. The mixture was stirred under reflux until ca. 7 ml of water had been collected (over a 3 h period). On cooling, brown blocks crystallized. The product was filtered off, washed with pentane and the mother liquor was evaporated under reduced pressure to afford a second crop of product. Yield 73 g (92%); m.p. 136 °C; MS(CI/NH_3), $m/z=176$ (M^+); HRMS for $C_9H_8N_2O_2$: 176.0586; Anal. Found: 176.0576. IR 3309 (ν N–H), 3125, 3111, 2993 (ν C–H), 2210 (ν C≡N), 1697 (δ C=O), 1582 (δ N–H), 1442, 1428, 1368, 1295, 1281, 1447, 1052, 1024, 890, 751, 701, 598. ^{1}H NMR ($CDCl_3$) d 3.89 (3H, s, CH_3O), 6.45 (1H, m, *H*C–pyrrole), 6.98 (1H, br, *H*C–pyrrole), 8.04 (1H, s, *H*C=C), 9.98 (1H, s, *H*N–pyrrole). ^{13}C NMR ($CDCl_3$) d 52.9 (*C*H_3O), 91.3 (*C*H=C), 112.6 (*C*=CH), 118.5 (*C*≡N), 124.6, 126.8, 128.8, 142.8 (*C*–pyrrole), 164.1 (*C*O_2CH_3). Anal. Calc. for $C_9H_8N_2O_3$: C, 61.35; H, 4.59; N, 15.90. Found: C, 61.38; H, 4.60; N, 15.81%.

2,2′-Benzyl-[5,5′-bis(2-cyano-2-methoxycarbonylvinyl)]dipyrrole (**4**). The protected pyrrole (**3**) (8.6 g, 0.0453 mol), benzaldehyde (9.3 g, 0.0877 mol), and a catalytic amount of *p*-toluene sulfonic acid (0.025 g) were refluxed in benzene (150 ml) in a round bottomed flask fitted with a Dean Stark trap for 6 h. The mixture was cooled, and the yellow product (**4**) was filtered off, washed with benzene (1 × 10 ml) and hexane (3 × 10 ml). The yellow powder was recrystallized from ethyl acetate. Yield 6.75 g (64% based on pyrrole); m.p. 110–112 °C; MS(CI/NH_3), $m/z=$ 440 (M^+); HRMS for $C_{25}H_{20}N_4O_4$: 440.1485; Anal. Found: 440.1483. IR 3265 (ν N–H), 3222 (ν C–H), 2215 (ν C≡N), 1680 (δ C=O), 1597, 1578 (δ N–H), 1473, 1427, 1406, 1292, 1200, 1096, 1058, 808, 761, 757, 737, 694 ^{1}H NMR (acetone-d^6) d 3.84 (6H, s, C*H*$_3$O), 5.64 (1H, s, *H*C–C_6H_5), 6.24 (2H, m, *H*C–pyrrole), 6.98 (2H, br, *H*C–pyrrole), 7.25, 7.41 (5H, m, *H*C–phenyl), 7.92 (2H, s, *H*C=C), 9.62 (2H, br, N*H*). ^{13}C NMR (acetone-d^6) d 45.1 (*C*H–C_6H_5), 53.2 (*C*H_3O), 92.8 (*C*H=C), 114.2 (*C*=CH), 118.0 (*C*≡N), 120.1, 127.9, 142.8, 143.3 (*C*–pyrrole),

128.6, 129.5, 130.0, 141.0 (*C*–phenyl), 164.9 (CO_2CH_3). Anal. Calc. for $C_{25}H_{20}N_4O_4$: C, 68.15; H, 4.58; N, 12.74. Found: C, 68.51; H, 4.58; N, 12.50%.

2,2′-Benzyl-5,5′-diformyl dipyrrole (**5**). The protected dipyrromethane (**4**) (1.3 g, 2.8 mmol) was suspended in aqueous CH_3OH solution (35% H_2O, 90 ml) of NaOH (6.78 g, 0.17 mol) in a 250 ml three-necked round bottomed flask under nitrogen. The solution immediately turned a deep green color, and the mixture was refluxed for 0.5 h. The CH_3OH was then removed by a slow distillation, maintaining the volume with addition of water, followed by cooling to room temperature. The product was extracted with CH_2Cl_2 (3×15 ml) and the combined extracts dried over $MgSO_4$. Evaporation of the solvent at reduced pressure gave an oil, from which buff colored blocky crystals formed on addition of a little ethyl acetate. Recrystallization from ethyl acetate/methylene chloride gave pale cream colored crystals. Yield 0.4 g (52%); m.p. 82–83 °C decomp.; MS(CI/NH_3), $m/z=278$ (M^+); HRMS for $C_{17}H_{14}N_2O_2$: 278.1054; Anal. Found: 278.1045. IR 3303–3172 (ν H_2O), 3142 (ν N–H), 3099 (ν Ar–H), 3032, 2964 (ν C–H), 2878, 2845 (ν H–CO), 1652 (δ C=O), 1560 (δ N–H), 1488, 1449, 1429, 1411, 1272, 1177, 1040, 821, 808, 771, 727, 699. ^{1}H NMR ($CDCl_3$) d 5.60 (1H, s, *H*C–C_6H_5), 6.07 (2H, d, *H*C–pyrrole), 6.88 (2H, d, *H*C–pyrrole), 7.30 (5H, m, *H*C–phenyl), 9.18 (2H, s, C*H*O), 10.98 (2H, br, N*H*). ^{13}C NMR ($CDCl_3$) d 44.5 (*C*H–C_6H_5), 111.6, 122.4, 139.2, 141.8 (*C*–pyrrole), 127.7, 128.5, 129.0, 132.7 (*C*–phenyl), 179.0 (*C*HO). Anal. Calc. for $C_{17}H_{14}N_2O_2$: C, 73.37; H, 5.07; N, 10.07. Found: C, 73.46; H, 4.99; N, 9.69%.

5.2.2. *Synthesis of [M(II)$_2$·2] complexes*

1,3-Diaminopropane (0.036 g, 0.480 mmol), the diformyldipyrromethane (**5**) (0.133 g, 0.480 mmol), and metal acetate (0.114 g, 0.480 mmol) were heated between 40 and 50 °C in absolute ethanol (25 ml) for 16 h. For the copper(II) and manganese(II) complexes, the ethanol was removed under reduced pressure, and the residue was recrystallized from methylene chloride/hexane to give a precipitate, which was filtered and dried. For the nickel complex, the product precipitated during the reaction, was filtered and washed twice with hexane (2×20 ml) to obtain pure product.

5.2.3. *Analysis of macrocyclic complexes*

[Mn(II)·**2**]$(CH_3CO_2)_2$. Yield 0.24 g (57%); MS (FAB in NBA) 736 (M^+) 794 ($M^+ + CH_3CO_2^-$). Anal. Calc. for $C_{40}H_{34}N_8Mn_2 \cdot 2CH_3CO_2 \cdot 2H_2O$: C, 59.32; H, 4.98; N, 12.58. Found: C, 59.16; H, 4.65; N, 12.29%. UV–vis λ_{max}(log ϵ): 290(4.63); 542(4.47); 5.68(4.41).

[Cu(II)·**2**]$(CH_3CO_2)_2$. Yield 0.28 g (63%); MS (FAB in NBA) 753 (M^+); 774 ($M^+ + O$); 811 ($M^+ + CH_3CO_2^-$). Anal. Calc. for $C_{40}H_{34}N_8Cu_2 \cdot 2CH_3CO_2 \cdot 3H_2O$: C, 57.07; H, 5.01; N, 12.10. Found: C, 56.97; H, 5.24; N, 12.10%. UV–vis λ_{max}(log ϵ): 323(4.40); 360(4.34); 552(3.93); 590(3.92).

[Ni(II)·**2**]. Yield 0.28 g (76%); MS (FAB in NBA) 753 (M^+); 774 ($M^+ + O$); 811 ($M^+ + CH_3CO_2^-$). Anal. Calc. for $C_{40}H_{34}N_8Ni_2 \cdot CH_3OH$: C, 63.44; H, 4.93; N,

14.44. Found: C, 63.70; H, 4.86; N, 14.15%. UV–vis $\lambda_{max}(\log \epsilon)$: 326(4.57); 432(3.94).

5.3. Monooxygenase studies

5.3.1. Oxidation of cyclohexene

Cyclohexene oxidations were carried out by placing iodosylbenzene (0.040 g, 0.18 mmol) and catalyst (0.01 mmol) in a Schlenk flask, which was evacuated and flushed with either nitrogen or argon three times. The glass stopper was then replaced with a rubber septum under inert gas. CH_2Cl_2 (5 ml), cyclopentanone (10 μl), and cyclohexene (10 μl) were syringed into the Schlenk flask. The mixture was stirred for 4 h and analyzed by GC. The products were determined by GC mass spectrometry and retention time in comparison to cyclopentanone as the internal standard. Yields are based on substrate added.

5.3.2. Oxidation of cis- and trans-stilbene

The procedure for oxidation of *cis*- and *trans*-stilbene was similar to that performed for the oxidation of cyclohexene. The solution mixture was stirred for 2 h in a Schlenk flask. The reaction was quenched with 10% (w/v) $NaHSO_3$ (300 ml) and stirred for an additional 10 min. The solvent was removed under reduced pressure to give either a solid or an oily product. The product was then stirred in hexane for 10 min. The hexane was removed under reduced pressure, and the residue was dissolved in $CDCl_3$ and analyzed by NMR.

Acknowledgements

The authors thank Larry Seib and Professor Fusao Takusagawa of the X-ray Crystallography Laboratory for the crystal structure data, and Dr. Todd Williams of the Mass Spectrometry Laboratory for mass spectral support. This work was funded by the National Institutes of Health GM 37577, the American Heart Association KS-93-GS-38, and the National Science Foundation EPSCoR Program.

References

[1] T.G. Spiro (Ed.), Metal Ion Activation of Dioxygen, Wiley-Interscience, New York, 1980.
[2] L. Que Jr. (Ed.), Metal Clusters in Proteins, ACS Symposium Series 372, American Chemical Society, Washington, D.C., 1988.
[3] L. Que Jr., A.E. True, Progr. Inorg. Chem.: Bioinorg. Chem. 38 (1990) 97.
[4] L. Que Jr., Y. Dong, Acc. Chem. Res. 29 (1996) 190.
[5] J.S. Valentine, C.S. Foote, A. Greenberg, J.F. Liebman (Eds.), Active Oxygen in Biochemistry, Chapman and Hall, London, 1995.
[6] K.D. Karlin, Science 261 (1993) 701 and references cited therein
[7] G.C. Dismukes, Chem. Rev. 96 (1996) 2909 and references cited therein
[8] K. Wieghardt, Angew. Chem., Int. Ed. Engl. 28 (1989) 1153 and references cited therein

[9] R.N. Mukherjee, Curr. Sci. 72 (1997) 802 and references cited therein
[10] C.L. Hill (Ed.), Activation and Functionalization of Alkanes, Wiley, New York, 1989.
[11] D.R.H. Barton, D. Doller, Acc. Chem. Res. 25 (1992) 504 and references cited therein
[12] P. Ortiz de Montellano (Ed.), Cytochrome P-450: Structure, Mechanism, and Biochemistry, Plenum Press, New York, 1985.
[13] V. Ullrich, Top. Curr. Chem. 83 (1979) 67 and references cited therein
[14] R. Raag, T.L. Poulos, Biochemistry 28 (1989) 917 and references cited therein
[15] B. Meunier, Chem. Rev. 92 (1992) 1411 and references cited therein
[16] E.I. Solomon, U.M. Sundaram, T.E. Machonkin, Chem. Rev. 96 (1996) 2563 and references cited therein
[17] J.D. Lipscomb, Ann. Rev. Microbiol. 48 (1994) 371 and references cited therein
[18] S.T. Longa, I. Ascone, A. Bianconi, A. Bonfigli, A.C. Castellano, O. Zarivi, M. Miranda, J. Biol. Chem. 271 (1996) 21025.
[19] A.C. Rosenzweig, C.A. Frederick, S.J. Lippard, P. Nordlund, Nature 366 (1993) 537.
[20] A.C. Rosenzweig, P. Nordlund, P.M. Takahara, C.A. Frederick, S.J. Lippard, Chem. Biol. 2 (1995) 409.
[21] M. Atta, P. Nordlund, A. Åberg, H. Eklund, M. Fontecave, J. Biol. Chem. 267 (1992) 20682.
[22] P. Nordlund, H. Eklund, J. Mol. Biol. 232 (1993) 123.
[23] R.G. Wilkins, Chem. Soc. Rev. (1992) 171.
[24] R.L. Rardin, W.B. Tolman, S.J. Lippard, New J. Chem. 15 (1991) 417.
[25] F.V. Acholla, K.B. Mertes, Tetrahedron Lett. 25 (1984) 3269.
[26] F.V. Acholla, F. Takusagawa, K.B. Mertes, J. Am. Chem. Soc. 107 (1985) 6902.
[27] F.V. Acholla, K.B. Mertes, Bull. Chem. Soc. Ethiop. 2 (1988) 73.
[28] F.V. Acholla, K.B. Mertes, Bull. Chem. Soc. Ethiop. 3 (1989) 17.
[29] J.B. Paine, III, D. Dolphin, J. Org. Chem. 53 (1988) 2787.
[30] J.B. Paine, III, R.B. Woodward, D. Dolphin, J. Org. Chem. 41 (1976) 2826.
[31] J.L. Sessler, J. Hugdahl, M.R. Johnson, J. Org. Chem. 51 (1986) 2838.
[32] T. Deffo, N. Gerasimchuk, O. Gerasimchuk, 1994.
[33] Y. Murakami, K. Sakata, D. Harada, Y. Matsuda, Bull. Chem. Soc. Jpn. 47 (1974) 3021.
[34] F.C. March, J.E. Fergusson, W.T. Robinson, J. Chem. Soc., Dalton Trans. (1972) 2069.
[35] J.W. Buchler, K.L. Lay, P.D. Smith, W.R. Scheidt, G.A. Rupprecht, J.E. Kenny, J. Organomet. Chem. 110 (1976) 109.
[36] J.T. Groves, T.E. Nemo, J. Am. Chem. Soc. 105 (1983) 5786.
[37] J.D. Koola, J.K. Kochi, Inorg. Chem. 26 (1987) 908.
[38] J.F. Kinneary, T.R. Wagler, C.J. Burrows, Tetrahedron Lett. 29 (1988) 877.
[39] C.-M. Che, W.-K. Cheng, J. Chem. Soc., Chem. Commun. (1986) 1443.
[40] K. Srinivasan, P. Michaud, J.K. Kochi, J. Am. Chem. Soc. 108 (1986) 2309.
[41] A.F. Tai, L.D. Margerum, J.S. Valentine, J. Am. Chem. Soc. 108 (1986) 5006.
[42] J.T. Groves, M.K. Stern, J. Am. Chem. Soc. 109 (1987) 3812.
[43] S. Banfi, M. Cavazzini, F. Coppa, S.V. Barkanova, O.L. Kaliya, J. Chem. Soc., Perkin Trans. II (1997) 1577.
[44] B.W. Schardt, F.J. Hollander, C.L. Hill, J. Am. Chem. Soc. 104 (1982) 3964.
[45] J.A. Smegal, B.C. Schardt, C.L. Hill, J. Am. Chem. Soc. 105 (1982) 3510.
[46] H.J. Lucas, E.R. Kennedy, Organic Synthesis, vol. 3, Wiley, New York, 1955, p. 482.